

Note on Thermalization of Non-resonantly Produced Sterile Neutrinos

Graciela B. Gelmini,^a Philip Lu^a and Volodymyr Takhistov^a

^a*Department of Physics and Astronomy, University of California, Los Angeles
Los Angeles, CA 90095-1547, USA*

E-mail: gelmini@physics.ucla.edu, philiplu11@gmail.com,
vtakhist@physics.ucla.edu

Abstract: In this addendum to the article JCAP 1912 (2019) no.12, 047 (arXiv:1909.13328) on the cosmological dependence of non-resonantly produced sterile neutrinos we discuss, using an analytic treatment, the parameter regions of large active-sterile neutrino mixing angles where sterile neutrinos can approach thermalization. We show that these additional considerations affect only large active-sterile neutrino mixing already rejected by different limits. Hence, the allowed sterile neutrino parameter regions are unaffected.

Contents

1	Introduction	1
2	Approaching Thermalization	2
3	Thermalization	5
4	Concluding Remarks	9
	Acknowledgments	9

1 Introduction

In Ref. [1] (from here on Paper I), as well as in its prior abbreviated companion paper [2], we have considered the cosmological dependence of non-resonantly produced sterile neutrinos. We discussed there the sensitivity of sterile neutrino production to cosmologies that differ from the standard radiation dominated cosmology (STD) before Big Bang Nucleosynthesis (BBN), specifically before the temperature of the Universe was 5 MeV. Alternative cosmologies can often appear in motivated theories. As examples, we have considered two distinct Scalar-Tensor models (ST1 [3] and ST2 [4]), Kination (K) [5–9] as well as Low Reheating Temperature (LRT) scenario [10–13], besides STD cosmology (see Paper I for a detailed description). We discussed how the resulting limits and regions of interest in the mass-mixing ($m_x, \sin^2 2\theta$) plane are affected for a sterile neutrino of mass m_x that is assumed to have a mixing $\sin \theta$ only with the active electron neutrino.

In Paper I we presented a simplified treatment of sterile neutrino production for the parameter region where mixing angles are very large. There, the momentum \vec{p} distribution $f_{\nu_s}(E, T)$ of sterile neutrinos of energy $E = |\vec{p}|$, which are relativistic at production temperature T , is not much smaller than the distribution of active neutrinos $f_{\nu_\alpha}(E, T)$. In part of this region sterile neutrinos can thermalize in the Early Universe, so that $f_{\nu_s}(E, T) = f_{\nu_\alpha}(E, T)$. When thermalized, sterile neutrinos have the same number density of one active neutrino species, i.e. during BBN and later $\Delta N_{\text{eff}} = 1$ (or close to 1, depending on entropy dilution), a value that is forbidden by present cosmological limits. In this addendum we analyze these effects.

We show, always using analytic expressions as in our previous studies, that the regions allowed by all sterile neutrino bounds are not affected by the present considerations.

2 Approaching Thermalization

In our analysis of Paper I, we assumed $f_{\nu_s} \ll f_{\nu_\alpha}$ and thus neglected the second term on the right hand side of the Boltzmann equation

$$\left(\frac{\partial f_{\nu_s}(E, T)}{\partial T} \right)_{\epsilon=E/T} = - \frac{\Gamma_s(E, T)}{HT} [f_{\nu_\alpha}(E, T) - f_{\nu_s}(E, T)] , \quad (2.1)$$

where H is the expansion rate of the Universe (see Eqs. (2.1), (2.3) to (2.5) and Fig. 1 of Paper I), $\Gamma_s(E, T)$ is the conversion rate of active to sterile neutrinos (see Eqs. (3.4) to (3.7) of Paper I), $\epsilon = E/T = |\vec{p}|/T$ is the T -scaled dimensionless momentum and the derivative on the left hand side is computed at constant ϵ . This equation assumes $f_{\nu_s}, f_{\nu_\alpha} \ll 1$. Neglecting f_{ν_s} on the right hand side amounts to neglecting the inverse oscillation process $\nu_s \rightarrow \nu_\alpha$. This is a good approximation for most of the large parameter space we studied with our analytic methods, $0.01 \text{ eV} < m_s < 1 \text{ MeV}$ and $10^{-13} < \sin^2 2\theta < 1$. However, the approximation fails for very large mixing angles, for which sterile neutrinos thermalize, thus $f_{\nu_s} = f_{\nu_\alpha}$ and the right hand side of Eq. (2.1) vanishes.

The way in which f_{ν_s} approaches f_{ν_α} with increasing mixing angle is quantified by the solution $f_{\nu_s-\text{nl}}$ to Eq. (2.1) [14]

$$f_{\nu_s-\text{nl}}(\epsilon, T) = \left(1 - e^{-K(\epsilon, T)} \right) f_{\nu_\alpha} = \left[1 - \exp \left(- \frac{f_{\nu_s-\text{lin}}(\epsilon, T)}{f_{\nu_\alpha}(\epsilon)} \right) \right] f_{\nu_\alpha}(\epsilon) . \quad (2.2)$$

We call this solution “non-linear”, $f_{\nu_s-\text{nl}}$, to distinguish it from the “linear” solution, $f_{\nu_s-\text{lin}}$, of the Boltzmann equation without f_{ν_s} on the right hand side. The solutions $f_{\nu_s-\text{lin}}$ for the different cases we studied are presented in detail in Paper I. Here, $K(\epsilon, T)$ is defined as

$$K(\epsilon, T) = \int_T^\infty dT \left(\frac{\Gamma_s(\epsilon, T)}{HT} \right)_\epsilon = \frac{f_{\nu_s-\text{lin}}(\epsilon, T)}{f_{\nu_\alpha}(\epsilon)} , \quad (2.3)$$

for all the cosmologies we consider except LRT for which the upper limit of integration is a finite constant temperature T_{RH} (see below). Notice that the integral is performed while keeping ϵ constant. We assume that there are no sterile neutrinos present before non-resonant production takes place. Eq. (2.2) can be easily verified to be the solution to Eq. (2.1) by substitution. Our previous solution is readily recovered as $f_{\nu_s-\text{lin}}$ becomes much smaller than f_{ν_α} and we then keep only the first non-trivial term in the exponential.

Eq. (2.3) corresponds to Eq. (3.10) of Paper I, except that in Paper I we approximated the lower limit of integration with $T = 0$. This is justified as the temperatures of interest are much lower than the temperature T_{max} at which the sterile neutrino production rate $(\partial f_{\nu_s}/\partial T)_\epsilon$ (neglecting f_{ν_s} in the right hand side of Eq. (2.1)) has a sharp maximum. For the STD cosmology, T_{max} is

$$T_{\text{max}}^{\text{STD}} = 145 \text{ MeV} \left(\frac{m_s}{\text{keV}} \right)^{\frac{1}{3}} \epsilon^{-\frac{1}{3}} , \quad (2.4)$$

and it is similar in the K, ST1 and ST2 cosmologies (see Eqs. (3.8), (3.9), (A.2) and (A.3) of Paper I). Hence, $f_{\nu_s-\text{lin}}$ becomes a function of ϵ only. This is a good approximation for the STD, ST1, ST2 and K cosmologies for which the solutions $f_{\nu_s-\text{lin}}(\epsilon)$ can be found in Eqs. (3.12), (3.13), (A.6) and (A.5) of Paper I, respectively.

In the LRT model, all of the sterile neutrino production is assumed to occur only during the late standard cosmology phase, at $T < T_{\text{RH}}$ below the reheating temperature. Thus, the upper limit of integration in Eq. (2.3) becomes T_{RH} . As the maximum of the production happens very close to T_{RH} , the lower limit of integration can again be taken to be $T = 0$, and in this case $f_{\nu_s-\text{lin}}(\epsilon)$ is given in Eq. (A.7) of Paper I.

Notice that $f_{\nu_s-\text{nl}}$ in Eq. (2.2) approaches the active neutrino distribution as the linear solution $f_{\nu_s-\text{lin}}$ grows larger than f_{ν_α} . This is a non-physical solution of the Boltzmann equation due to not taking into account f_{ν_s} on the right hand side.

As we will now show, the function $f_{\nu_s-\text{nl}}$ departs significantly from the linear solution $f_{\nu_s-\text{lin}}$ given in Paper I for mixing angles that are forbidden by the dark matter density condition $\Omega_s < \Omega_{\text{DM}}$ and by the upper limit $N_{\text{eff}} < 3.4$ on the effective number of relativistic active neutrino species present during BBN. As these regions are already forbidden, the resulting limits of Paper I are unaffected.

In order to derive all limits that depend on the sterile neutrino number density n_{ν_s} , one needs to integrate $f_{\nu_s-\text{nl}}$ over momenta to obtain n_{ν_s} . Following our previous notation we will denote the integration result as “non-linear” number density $n_{\nu_s-\text{nl}}$, and the number densities we presented before in Paper I as “linear” $n_{\nu_s-\text{lin}}$. The integration needs to be performed numerically, unless the ratio $(f_{\nu_s-\text{lin}}/f_{\nu_\alpha})$ is a constant independent of ϵ . This is the case for the STD and ST2 cosmologies, where

$$\left(\frac{n_{\nu_s-\text{lin}}}{n_{\nu_\alpha}} \right) = \left(\frac{f_{\nu_s-\text{lin}}}{f_{\nu_\alpha}} \right) \quad (2.5)$$

and we can obtain the exact solution for $n_{\nu_s-\text{nl}}$,

$$\left(\frac{n_{\nu_s-\text{nl}}}{n_{\nu_\alpha}} \right) = 1 - e^{-(n_{\nu_s-\text{lin}}/n_{\nu_\alpha})} . \quad (2.6)$$

Following our analysis of Paper I, we will proceed with an analytic treatment. We are going to find approximate analytic solutions for $n_{\nu_s-\text{nl}}$ for the other cosmologies we consider in which Eq. (2.5) does not hold, because the ratio $(f_{\nu_s-\text{lin}}/f_{\nu_\alpha})$ depends on ϵ . The exact solution would require integration over momentum of an exponential function of ϵ . Since the dependence of the $(f_{\nu_s-\text{lin}}/f_{\nu_\alpha})$ ratio on ϵ is weak, our approximation is justified.

With the dark matter abundance $\Omega_{\text{DM}} h^2 = 0.12$, a fully thermalized sterile neutrino, with the relic number density of an active neutrino species, would constitute all of dark matter if its mass is $m_s = 11.5$ eV. Thus, there is no dark matter density bound for lighter sterile neutrinos, when $m_s < 11.5$ eV, since the number density of sterile neutrinos is at most equal to that of one active neutrino. Above and close to this limiting mass value, taking into

account the non-linear solution $f_{\nu_s-\text{nl}}$ modifies the dark matter density limit with respect to the results of Paper I.

In order to find an approximate analytic solution for $n_{\nu_s-\text{nl}}$, let us start by defining a pre-factor C such that Eq. (A.10) of Ref. [15] for the sterile neutrino relic number density is

$$n_{\nu_s-\text{lin}} = C \sin^2 2\theta \quad (2.7)$$

(i.e. C includes all the factors independent of the active-sterile mixing angle). When the density of sterile neutrinos accounts for all of the dark matter, i.e. when $\rho_{\nu_s} = \rho_{\text{DM}}$, the non-linear solution for the number density satisfies

$$\rho_{\text{DM}} = m_s n_{\nu_s-\text{nl}} = 11.5 \text{ eV } n_{\nu_\alpha} . \quad (2.8)$$

We denote dark matter density limit obtained using $n_{\nu_s-\text{lin}}$, as in Paper I, as $(\sin^2 2\theta)_{\text{old}}$ that is a function of m_s . Thus, we can now state Eq. (A.25) of Paper I for the dark matter fraction in sterile neutrinos for the K and ST2 cosmologies (or specifically Eqs. (A.26) and (A.27)) and Eq. (A.28) for the same fraction for the LRT model, setting these fractions to 1, as

$$1 = \frac{n_{\nu_s-\text{lin}} m_s}{\rho_{\text{DM}}} = \frac{C(\sin^2 2\theta)_{\text{old}} m_s}{\rho_{\text{DM}}} . \quad (2.9)$$

Using Eqs. (2.7), (2.8) and (2.9) we can relate $n_{\nu_s-\text{nl}}$ with the Paper I dark matter limit $(\sin^2 2\theta)_{\text{old}}$,

$$\frac{C(\sin^2 2\theta)_{\text{old}}}{n_{\nu_\alpha}} = \frac{\rho_{\text{DM}}}{m_s n_{\nu_\alpha}} = \frac{11.5 \text{ eV}}{m_s} = \frac{n_{\nu_s-\text{nl}}}{n_{\nu_\alpha}} . \quad (2.10)$$

This allows to define $(\sin^2 2\theta)_{\text{new}}$ such that the ratio $(n_{\nu_s-\text{nl}}/n_{\nu_\alpha})$ in Eq. (2.6) satisfies Eq. (2.10) when $(\sin^2 2\theta)_{\text{new}}$ is used in $n_{\nu_s-\text{lin}}$ in the exponent in the same equation, so that $(n_{\nu_s-\text{nl}}/n_{\nu_\alpha}) = 11.5 \text{ eV}/m_s$. Hence,

$$\frac{11.5 \text{ eV}}{m_s} = 1 - \exp \left(- \frac{C(\sin^2 2\theta)_{\text{new}}}{n_{\nu_\alpha}} \right) . \quad (2.11)$$

Replacing here n_{ν_α} by $C(\sin^2 2\theta)_{\text{old}} m_s / 11.5 \text{ eV}$ using Eq. (2.10), the Eq. (2.11) can be rearranged to give the new mixing angle for the dark matter density limit (plotted in the figures) in terms of the old mixing angle (see Eqs. (A.29) to (A.32) of Paper I)

$$(\sin^2 2\theta)_{\text{new}} = (\sin^2 2\theta)_{\text{old}} \frac{m_s}{11.5 \text{ eV}} \ln \left[\frac{m_s}{m_s - 11.5 \text{ eV}} \right] . \quad (2.12)$$

This is the boundary of the dark gray regions where $\Omega_s > \Omega_{\text{DM}}$ shown in Fig. 1 and Fig. 2. Except in a region close to or below $m_s = 11.5 \text{ eV}$, which is rejected by the (cyan) N_{eff} BBN limit, the present dark matter density limits are the same as those in Paper I. Thus the allowed regions have not changed.

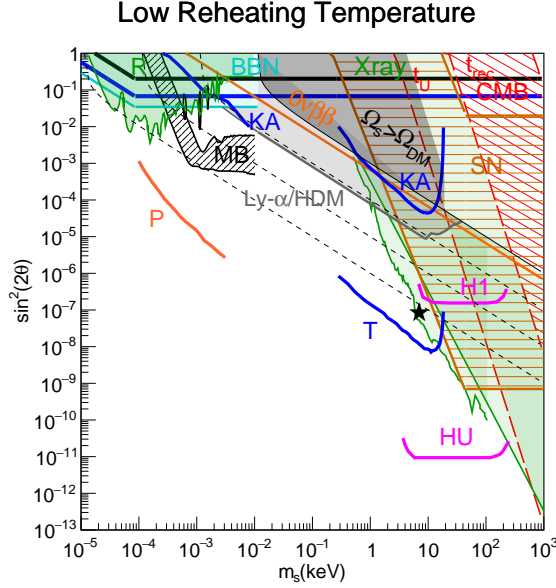


Figure 1: Present relic abundance, limits and regions of interest in the mass-mixing space of a ν_s mixed with ν_e , for the LRT cosmology with $T_{\text{RH}} = 5$ MeV [10]. $g_* = 10.75$ is used for $m_s < 11.5$ eV, and $g_* = 30$ above. Shown are the fraction of the DM in ν_s of 1 (black solid line) and 10^{-1} , 10^{-2} and 10^{-3} (black dotted lines), the forbidden region $\Omega_s/\Omega_{\text{DM}} > 1$ (shaded in dark gray), lifetimes $\tau = t_U$, t_{rec} and t_{th} of Majorana ν_s (straight long dashed red lines), the region (SN) disfavored by supernovae [16] (horizontally hatched in brown), the location of the 3.5 keV X-ray signal [17, 18] (black star). The regions rejected by reactor neutrino (R) experiments (Daya Bay [19], Bugey-3 [20] and PROSPECT [21]) shown in green, limits on N_{eff} during BBN [22] (BBN) in cyan, Lyman-alpha limits [23] (Ly- α /HDM) shaded in light gray, X-ray limits [24–26] including DEBRA [27] (Xray) in green, $0\nu\beta\beta$ decays [28] ($0\nu\beta\beta$) in orange and CMB spectrum distortions [29] (CMB) diagonally hatched in red. Current/future sensitivity of KATRIN (KA) in the keV [30] and eV [31] mass range, its TRISTAN upgrade in 3 yr (T) [30] shown by blue solid lines. Magenta solid lines show the reach of the phase 1A (H1) of HUNTER, and its upgrade (HU) [32]. The 4- σ band of compatibility with LSND and MiniBooNE results (MB) in Fig. 4 of [33] is shown densely hatched in black. The three black vertical elliptical contours are the regions allowed at 3- σ by DANSS [34] and NEOS [35] data in Fig. 4 of [36]. Orange solid lines show the reach of PTOLEMY for 100 g-yr (P) exposure (from Figs. 6 and 7 of [37]). See Paper I for details. The thick blue line represents the thermalization condition $f_{\nu_s-\text{lin}} = f_{\nu_\alpha}$ and the thick black line shows $f_{\nu_s-\text{lin}} = 3f_{\nu_\alpha}$. Notice that the LRT model goes into the STD cosmology when T_{max} is not larger than $T_{\text{RH}} = 5$ MeV, i.e. for $m_s < 0.1$ eV.

3 Thermalization

The production of sterile neutrinos saturates when they thermalize, when $f_{\nu_s} = f_{\nu_\alpha}$, and thus the right hand side of the Boltzmann equation Eq. (2.1) is equal to zero. In Fig. 2, the

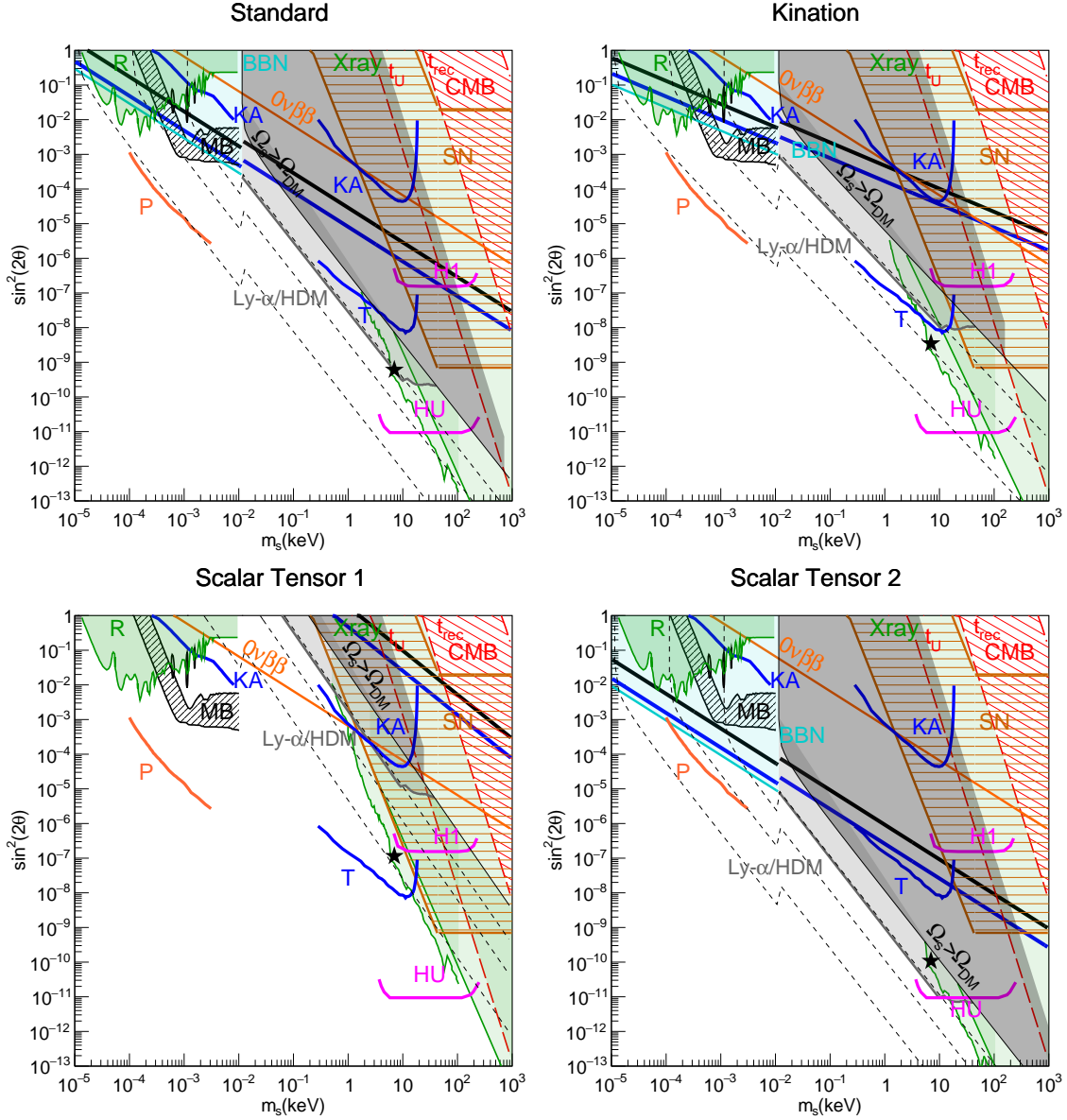


Figure 2: Present relic abundance, limits and regions of interest for standard, kination and scalar-tensor cosmologies. See caption in Fig. 1. Here the thick blue line represents the condition $\Gamma/H|_{T_{max}} = 1$ that coincides with $f_{\nu_s} = f_{\nu_\alpha}$ as in Fig. 1. The discontinuity in the limits is due to our use of just two values for g_* , 10.75 below and 30 above $m_s = 11.5$ eV (see explanations in the text).

region of thermalization where $\Gamma/H|_{T_{max}} \geq 1$ is demarcated with a solid blue line at its lower boundary. When the maximum production rate $\Gamma(T_{max})$ stays roughly equal to or larger than the Hubble parameter for a significant period of time, a substantial amount of sterile

neutrinos are produced and the population is nearly or fully thermalized.

To compute the production rates and momentum distributions we use as the characteristic momentum $\epsilon = \langle \epsilon \rangle$. $\langle \epsilon \rangle$ is the average value of E/T for each cosmology (see Eqs. (3.27) and (3.28) of Paper I)

$$\langle \epsilon \rangle = \begin{cases} 3.15, & \text{STD} \\ 3.47, & \text{K} \\ 2.89, & \text{ST1} \\ 3.15, & \text{ST2} \\ 4.11, & \text{LRT} \end{cases} \quad (3.1)$$

In contrast to Paper I, except for LRT we use two values of the effective number of degrees of freedom contributing to the radiation density in H , $g_* = 10.75$ for $m_s < 11.5$ eV and $g_* = 30$ for $m_s > 11.5$ eV. This choice allows to better approximate the evolution of g_* with temperature [38–40]. We have chosen $m_s = 11.5$ eV as the mass where g_* changes, because for this mass $T_{\text{max}} \simeq 20$ MeV and this is the temperature above which g_* starts increasing from its value of 10.75. In Paper I we had adopted for simplicity $g_* = 30$ throughout the entire mass range, except for the N_{eff} BBN limit, which is particularly relevant for light sterile neutrinos, and the LRT cosmology, for which we used 10.75. Here we instead adopt $g_* = 10.75$ for all our calculations with $m_s < 11.5$ eV as this value is more appropriate to the sterile neutrino production and thermalization at the eV scale, specifically in the regions where possible LSND, MiniBooNE, DANSS and NEOS sterile neutrino detection signals have been suggested. Our choice of using two distinct values of g_* results in an artificial discontinuity¹ in all the limits in Fig. 2. In the LRT cosmology, production happens only at $T < 5$ MeV, for which $g_* = 10.75$, for all sterile neutrinos. Thus there are no discontinuities in the limits in Fig. 1.

We note that the LRT model assumes that T_{max} is larger than $T_{\text{RH}} = 5$ MeV, which is not true for $m_s < 0.1$ eV. For such small masses, the LRT model becomes just the STD cosmology. This is shown in Fig. 1, where in this low mass range all the LRT limits transition to those of the STD cosmology as in Fig. 2. This minor distinction had not been made in Paper I.

Solving for $\sin^2 2\theta$ from the condition $\Gamma/H|_{T_{\text{max}}} = 1$ we obtain the following limits (the solid blue lines in Fig. 2),

$$\text{for STD:} \quad (\sin^2 2\theta)_{\text{th}} = 4.86 \times 10^{-3} \left(\frac{d_\alpha}{1.27} \right)^{-1} \left(\frac{m_s}{\text{eV}} \right)^{-1} \left(\frac{g_*}{10.75} \right)^{\frac{1}{2}}, \quad (3.2)$$

$$\text{for K:} \quad (\sin^2 2\theta)_{\text{th}} = 1.52 \times 10^{-2} \epsilon^{-\frac{1}{3}} \left(\frac{d_\alpha}{1.27} \right)^{-1} \left(\frac{m_s}{\text{eV}} \right)^{-\frac{2}{3}} \left(\frac{g_*}{10.75} \right)^{\frac{1}{2}}, \quad (3.3)$$

$$\text{for ST1:} \quad (\sin^2 2\theta)_{\text{th}} = 1.38 \times 10^3 \epsilon^{0.27} \left(\frac{d_\alpha}{1.27} \right)^{-1} \left(\frac{m_s}{\text{eV}} \right)^{-1.27} \left(\frac{g_*}{10.75} \right)^{\frac{1}{2}}, \quad (3.4)$$

¹Had we instead considered the true value of g_* that is a continuous function of temperature, such discontinuity would be absent.

and for ST2: $(\sin^2 2\theta)_{\text{th}} = 1.56 \times 10^{-4} \left(\frac{d_\alpha}{1.27} \right)^{-1} \left(\frac{m_s}{\text{eV}} \right)^{-1} \left(\frac{g_*}{10.75} \right)^{\frac{1}{2}}.$ (3.5)

We have confirmed that these limits derived from $\Gamma/H|_{T_{\text{max}}} = 1$ practically coincide with those corresponding to $f_{\nu_s-\text{lin}} = f_{\nu_\alpha}$, which we thus do not display separately in Fig. 2.

For the LRT model, considering that the maximum production rate is at $T_{\text{RH}} = 5$ MeV, we could be tempted to use $\Gamma/H|_{T_{\text{RH}}} = 1$ as the condition for thermalization. However, when employing this condition throughout the whole range of integration in T , from 0 to T_{RH} , to obtain $K(\epsilon, T)$, the integrand is smaller than 1. Thus, this is not a good condition of thermalization for this model. Since in all the other models we consider the thermalization condition based on Γ/H coincides with the condition $f_{\nu_s-\text{lin}} = f_{\nu_\alpha}$, we thus adopt $f_{\nu_s-\text{lin}} = f_{\nu_\alpha}$ as the condition for thermalization in the LRT model. This condition translates into

$$(\sin^2 2\theta)_{\text{th}} = 2.78 \times 10^{-1} \epsilon^{-1}, \quad (3.6)$$

which is shown with the thick blue line in Fig. 1.

Notice that we have considered the condition $\Gamma/H > 1$ for chemical equilibrium of sterile neutrinos, since the rate Γ we used is the production rate. Kinetic equilibrium happens at larger mixing angles than chemical equilibrium. The reason for this is that the sterile neutrino scattering rate contains an extra $\sin^2 \theta$ factor over the production rate. Thus, sterile neutrinos that are not in chemical equilibrium (i.e. for which the production rate is $\Gamma < H$) are also not in kinetic equilibrium, they are decoupled from the thermal bath.

On the thick blue lines in the figures, $f_{\nu_s-\text{nl}} = (1 - e^{-1})f_{\nu_\alpha} = 0.63f_{\nu_\alpha}$. In Fig. 1 and Fig. 2 we also display with a solid black line where $f_{\nu_s-\text{lin}} = 3f_{\nu_\alpha}$, and thus $f_{\nu_s-\text{nl}} = (1 - e^{-3})f_{\nu_\alpha} = 0.95f_{\nu_\alpha}$, where nearly full thermalization occurs. Above this black line, the sterile neutrino momentum distribution rapidly becomes $f_{\nu_s} = f_{\nu_\alpha}$ with increased mixing (i.e. the right hand side of the Boltzmann equation Eq. (2.1) goes to zero). The equations of the thick black line in the figures are:

for STD: $\sin^2 2\theta = 1.73 \times 10^{-2} \left(\frac{d_\alpha}{1.27} \right)^{-1} \left(\frac{m_s}{\text{eV}} \right)^{-1} \left(\frac{g_*}{10.75} \right)^{\frac{1}{2}},$ (3.7)

for K: $\sin^2 2\theta = 4.29 \times 10^{-2} \epsilon^{-\frac{1}{3}} \left(\frac{d_\alpha}{1.27} \right)^{-1} \left(\frac{m_s}{\text{eV}} \right)^{-\frac{2}{3}} \left(\frac{g_*}{10.75} \right)^{\frac{1}{2}},$ (3.8)

for ST1: $\sin^2 2\theta = 5.27 \times 10^3 \epsilon^{0.27} \left(\frac{d_\alpha}{1.27} \right)^{-1} \left(\frac{m_s}{\text{eV}} \right)^{-1.27} \left(\frac{g_*}{10.75} \right)^{\frac{1}{2}},$ (3.9)

for ST2: $\sin^2 2\theta = 5.52 \times 10^{-4} \left(\frac{d_\alpha}{1.27} \right)^{-1} \left(\frac{m_s}{\text{eV}} \right)^{-1} \left(\frac{g_*}{10.75} \right)^{\frac{1}{2}},$ (3.10)

and for LRT: $\sin^2 2\theta = 8.34 \times 10^{-1} \epsilon^{-1}.$ (3.11)

Eqs. (2.5) and (2.6) imply that $f_{\nu_s-\text{lin}} = 3f_{\nu_\alpha}$ corresponds to $n_{\nu_s-\text{nl}}/n_{\nu_\alpha} \simeq 0.95$, which leads to $\rho_s = \rho_{\text{DM}}$ for $m_s = 11.5$ eV. In fact, in the figures the thick blue line intersects the dark

matter density limit near $m_s = 11.5$ eV, as expected.

4 Concluding Remarks

We have considered the approach of sterile neutrinos to thermalization that happens for large enough active-sterile mixing angles. We showed that the allowed regions of parameter space found in Paper I are not affected by these considerations. In particular, the interesting region in which there are several suggested potential signals of a light sterile neutrino with mass close to 1 eV are free from cosmological bounds in the ST1 and LRT cosmologies.

Acknowledgments

The work of G.B.G., P.L. and V.T. was supported in part by the U.S. Department of Energy (DOE) Grant No. DE-SC0009937.

References

- [1] G. B. Gelmini, P. Lu and V. Takhistov, *Cosmological Dependence of Non-resonantly Produced Sterile Neutrinos*, *JCAP* **12** (2019) 047 [[1909.13328](#)].
- [2] G. B. Gelmini, P. Lu and V. Takhistov, *Visible Sterile Neutrinos as the Earliest Relic Probes of Cosmology*, *Phys. Lett. B* **800** (2020) 135113 [[1909.04168](#)].
- [3] R. Catena, N. Fornengo, A. Masiero, M. Pietroni and F. Rosati, *Dark matter relic abundance and scalar - tensor dark energy*, *Phys. Rev.* **D70** (2004) 063519 [[astro-ph/0403614](#)].
- [4] R. Catena, N. Fornengo, A. Masiero, M. Pietroni and M. Schelke, *Enlarging $mSUGRA$ parameter space by decreasing pre-BBN Hubble rate in Scalar-Tensor Cosmologies*, *JHEP* **10** (2008) 003 [[0712.3173](#)].
- [5] B. Spokoiny, *Deflationary universe scenario*, *Phys. Lett.* **B315** (1993) 40 [[gr-qc/9306008](#)].
- [6] M. Joyce, *Electroweak Baryogenesis and the Expansion Rate of the Universe*, *Phys. Rev.* **D55** (1997) 1875 [[hep-ph/9606223](#)].
- [7] P. Salati, *Quintessence and the relic density of neutralinos*, *Phys. Lett.* **B571** (2003) 121 [[astro-ph/0207396](#)].
- [8] S. Profumo and P. Ullio, *SUSY dark matter and quintessence*, *JCAP* **0311** (2003) 006 [[hep-ph/0309220](#)].
- [9] C. Pallis, *Quintessential kination and cold dark matter abundance*, *JCAP* **0510** (2005) 015 [[hep-ph/0503080](#)].
- [10] G. Gelmini, S. Palomares-Ruiz and S. Pascoli, *Low reheating temperature and the visible sterile neutrino*, *Phys. Rev. Lett.* **93** (2004) 081302 [[astro-ph/0403323](#)].
- [11] G. B. Gelmini and P. Gondolo, *Neutralino with the right cold dark matter abundance in (almost) any supersymmetric model*, *Phys. Rev.* **D74** (2006) 023510 [[hep-ph/0602230](#)].
- [12] G. Gelmini, P. Gondolo, A. Soldatenko and C. E. Yaguna, *The Effect of a late decaying scalar on the neutralino relic density*, *Phys. Rev.* **D74** (2006) 083514 [[hep-ph/0605016](#)].

- [13] G. Gelmini, E. Osoba, S. Palomares-Ruiz and S. Pascoli, *MeV sterile neutrinos in low reheating temperature cosmological scenarios*, *JCAP* **0810** (2008) 029 [[0803.2735](#)].
- [14] T. Rehagen and G. B. Gelmini, *Effects of kination and scalar-tensor cosmologies on sterile neutrinos*, *JCAP* **1406** (2014) 044 [[1402.0607](#)].
- [15] G. B. Gelmini, P. Lu and V. Takhistov, *Cosmological Dependence of Resonantly Produced Sterile Neutrinos*, *JCAP* **06** (2020) 008 [[1911.03398](#)].
- [16] K. Kainulainen, J. Maalampi and J. T. Peltoniemi, *Inert neutrinos in supernovae*, *Nucl. Phys.* **B358** (1991) 435.
- [17] E. Bulbul, M. Markevitch, A. Foster, R. K. Smith, M. Loewenstein and S. W. Randall, *Detection of An Unidentified Emission Line in the Stacked X-ray spectrum of Galaxy Clusters*, *Astrophys. J.* **789** (2014) 13 [[1402.2301](#)].
- [18] A. Boyarsky, O. Ruchayskiy, D. Iakubovskiy and J. Franse, *Unidentified Line in X-Ray Spectra of the Andromeda Galaxy and Perseus Galaxy Cluster*, *Phys. Rev. Lett.* **113** (2014) 251301 [[1402.4119](#)].
- [19] DAYA BAY collaboration, F. P. An et al., *Improved Search for a Light Sterile Neutrino with the Full Configuration of the Daya Bay Experiment*, *Phys. Rev. Lett.* **117** (2016) 151802 [[1607.01174](#)].
- [20] Y. Declais et al., *Search for neutrino oscillations at 15-meters, 40-meters, and 95-meters from a nuclear power reactor at Bugey*, *Nucl. Phys.* **B434** (1995) 503.
- [21] PROSPECT collaboration, J. Ashenfelter et al., *First search for short-baseline neutrino oscillations at HFIR with PROSPECT*, *Phys. Rev. Lett.* **121** (2018) 251802 [[1806.02784](#)].
- [22] PARTICLE DATA GROUP collaboration, M. Tanabashi et al., *Review of Particle Physics*, *Phys. Rev.* **D98** (2018) 030001.
- [23] J. Baur, N. Palanque-Delabrouille, C. Yeche, A. Boyarsky, O. Ruchayskiy, E. Armengaud et al., *Constraints from Ly- α forests on non-thermal dark matter including resonantly-produced sterile neutrinos*, *JCAP* **1712** (2017) 013 [[1706.03118](#)].
- [24] K. C. Y. Ng, B. M. Roach, K. Perez, J. F. Beacom, S. Horiuchi, R. Krivonos et al., *New Constraints on Sterile Neutrino Dark Matter from NuSTAR M31 Observations*, *Phys. Rev.* **D99** (2019) 083005 [[1901.01262](#)].
- [25] K. Perez, K. C. Y. Ng, J. F. Beacom, C. Hersch, S. Horiuchi and R. Krivonos, *Almost closing the ν MSM sterile neutrino dark matter window with NuSTAR*, *Phys. Rev.* **D95** (2017) 123002 [[1609.00667](#)].
- [26] A. Neronov, D. Malyshev and D. Eckert, *Decaying dark matter search with NuSTAR deep sky observations*, *Phys. Rev.* **D94** (2016) 123504 [[1607.07328](#)].
- [27] A. Boyarsky, A. Neronov, O. Ruchayskiy and M. Shaposhnikov, *Constraints on sterile neutrino as a dark matter candidate from the diffuse x-ray background*, *Mon. Not. Roy. Astron. Soc.* **370** (2006) 213 [[astro-ph/0512509](#)].
- [28] KAMLAND-ZEN collaboration, A. Gando et al., *Search for Majorana Neutrinos near the Inverted Mass Hierarchy Region with KamLAND-Zen*, *Phys. Rev. Lett.* **117** (2016) 082503 [[1605.02889](#)].

- [29] D. J. Fixsen, E. S. Cheng, J. M. Gales, J. C. Mather, R. A. Shafer and E. L. Wright, *The Cosmic Microwave Background spectrum from the full COBE FIRAS data set*, *Astrophys. J.* **473** (1996) 576 [[astro-ph/9605054](#)].
- [30] KATRIN collaboration, S. Mertens et al., *A novel detector system for KATRIN to search for keV-scale sterile neutrinos*, *J. Phys.* **G46** (2019) 065203 [[1810.06711](#)].
- [31] KATRIN collaboration, F. Megas, *eV-scale Sterile Neutrino Investigation with the First Tritium KATRIN Data*, *Master's Thesis* .
- [32] P. F. Smith, *Proposed experiments to detect keV range sterile neutrinos using energy-momentum reconstruction of beta decay or K-capture events*, *New J. Phys.* **21** (2019) 053022 [[1607.06876](#)].
- [33] MINIBOONE collaboration, A. A. Aguilar-Arevalo et al., *Significant Excess of ElectronLike Events in the MiniBooNE Short-Baseline Neutrino Experiment*, *Phys. Rev. Lett.* **121** (2018) 221801 [[1805.12028](#)].
- [34] DANSS collaboration, I. Alekseev et al., *Search for sterile neutrinos at the DANSS experiment*, *Phys. Lett.* **B787** (2018) 56 [[1804.04046](#)].
- [35] NEOS collaboration, Y. J. Ko et al., *Sterile Neutrino Search at the NEOS Experiment*, *Phys. Rev. Lett.* **118** (2017) 121802 [[1610.05134](#)].
- [36] S. Gariazzo, C. Giunti, M. Laveder and Y. F. Li, *Model-independent $\bar{\nu}_e$ short-baseline oscillations from reactor spectral ratios*, *Phys. Lett.* **B782** (2018) 13 [[1801.06467](#)].
- [37] PTOLEMY collaboration, M. G. Betti et al., *Neutrino physics with the PTOLEMY project: active neutrino properties and the light sterile case*, *JCAP* **1907** (2019) 047 [[1902.05508](#)].
- [38] L. Husdal, *On Effective Degrees of Freedom in the Early Universe*, *Galaxies* **4** (2016) 78 [[1609.04979](#)].
- [39] S. Borsanyi et al., *Calculation of the axion mass based on high-temperature lattice quantum chromodynamics*, *Nature* **539** (2016) 69 [[1606.07494](#)].
- [40] M. Drees, F. Hajkarim and E. R. Schmitz, *The Effects of QCD Equation of State on the Relic Density of WIMP Dark Matter*, *JCAP* **1506** (2015) 025 [[1503.03513](#)].